RSC Advances

ROYAL SOCIETY OF CHEMISTRY

www.rsc.org/advances

Pyrolysis (fast and slow, catalytic and thermal) is explored for the conversion of spent coffee grounds into higher value chemicals.

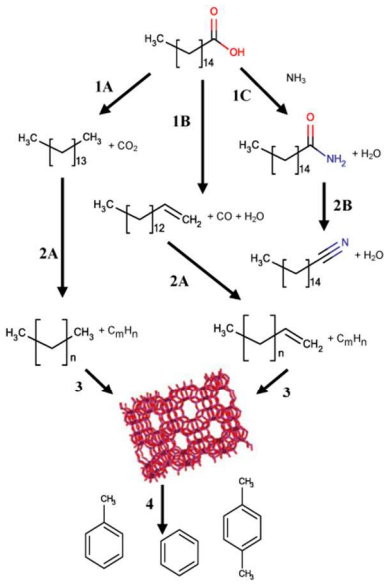

RSC Advances

RSCPublishing

ARTICLE

The effect of temperature, heating rate, and ZSM-5 catalyst on the product selectivity of the fast pyrolysis of Spent Coffee Grounds

Ari Fischer*, Shoucheng Du*, Julia A. Valla and George M. Bollas†

Cite this: DOI: 10.1039/xoxxoooooox

Received ooth January 2012,
Accepted ooth January 2012

DOI: 10.1039/xoxxoooooox

www.rsc.org/

Spent coffee grounds (SCG) are a continuously produced and abundant biomass resource that is rich in fixed carbon and underutilized. In this study, fast pyrolysis was employed as a method of upgrading this waste product into higher value chemicals and commodities. The effect of catalytic upgrading via a ZSM-5 catalyst on the pyrolysis product was investigated at two heating rates and three different pyrolysis temperatures. ZSM-5 catalyst was explored as the means to increase selectivity to deoxygenated olefins and aromatic products. The liquid products from the pyrolysis of SCG were predominantly fatty acids, linear hydrocarbons, furans, phenols, ketones, and aromatic hydrocarbons. The ZSM-5 catalyst was seen to decrease selectivity to linear hydrocarbons and furans, and enhance selectivity to aromatic hydrocarbons and CO. Increasing the pyrolysis temperature was seen to decrease selectivity to fatty acids, and increase selectivity to aromatic and linear hydrocarbons.

Introduction

The production of chemicals from spent coffee grounds (SCG) is a promising sustainable strategy for the valorization of this vast waste product. SCG fall into the general category of waste biomass, which is a renewable resource that has the potential to assist with energy generation and chemicals production.[1,2] The advantages of using SCG compared to more conventional biomass (e.g. woody biomass) include their established transportation, pleasant smell, stability, and low cost.[3] As with all waste biomass, production of chemical commodities from SCG can be accomplished without competing with the food and agriculture sectors. In addition, waste coffee is a good candidate for fuels and chemicals production due to its expansive and continuous supply. Coffee is the world's second largest traded commodity, second only to petroleum products, and its utilization generates vast amounts of waste because the beans are not entirely consumed during the coffee brewing. The International Coffee Organization[4] reported that over 4.2 million metric tons of coffee waste are generated annually (2013-2014 estimate) by countries who import coffee, which illustrates the scale of availability of this feedstock. After brewing, SCG typically end up in landfills. The main problem with disposing of SCG in landfills is that they take up large amounts of space, their fixed carbon content is wasted, and they are a source of methane emissions as a result of anaerobic decomposition.[5]

A variety of commercial and industrial applications for SCG have been explored in the literature, attempting to provide alternative uses for SCG. The use of SCG as an additive in animal feed was studied by Adams et al.,[6] who concluded that the anti-nutritional tannin and caffeine content limits the maximum coffee in ruminant feed to 10 wt%. The use of SCG in the spirits industry was explored by Sampaio et al.,[7] who developed a novel distilled beverage from SCG fermentation which contained 40 vol% ethanol and had a mild coffee flavor. The use of SCG in industrial purposes was explored by Silva et al.,[8] who reported that SCG are an excellent fuel source for on-site boilers in the soluble coffee industry. However, the particulate matter formed by combustion of SCG was reported as a drawback.[8] Gasification of SCG in a dual fluidized bed was explored by Xu et al.[9] A pilot plant operating at 5.0 kg/hr was able to convert up to 70 wt% of the carbon in the SCG feed into product gas with a higher heating value of 14500 kJ/m^3. The significant tar yield (up to 50 gr/m^3 of gas) from the gasification process was reported as a major drawback.[9]

Several recent studies have explored the use of SCG as a feedstock for biodiesel production, aiming to utilize its high lipid content (up to 27 wt%).[10] A study performed by Kondamudi et al.[3] synthesized biodiesel from lipids extracted from SCG. It was estimated that up to 340 million gallons of coffee-derived biodiesel could be added to the global fuel supply annually. Another exploration of SCG as a feedstock for biodiesel production was performed by Vardon et al.,[11] who

extracted lipids from SCG, which were subsequently used to synthesize biodiesel with an energy density of 39.6 MJ/kg. Due to its prohibitively high acidity, viscosity, and sulfur content, the SCG biodiesel did not meet the American Society for Testing and Materials (ASTM) fuel specifications.[11] Another disadvantage of using SCG for biodiesel production is that utilizing only the lipid content of SCG does not eliminate the solid waste problem.

As an alternative processing option, pyrolysis of SCG was performed by Bok et al.[12] in a fluidized-bed reactor that operated between 673-873 K with a rapid heating rate of 1000-10000 K/sec. The pyrolysis liquid yield was highest at 54.85 wt%, which was achieved at 823 K. The liquid product from SCG pyrolysis had a water content ranging from 23.96-32.93 wt%.[12] Other liquid products included ketones, phenols, furans, and caffeine. Slow pyrolysis of SCG was performed by Vardon et al.[11] who compared the pyrolysis of SCG and the defatted SCG at 723 K with a heating rate of 50 K/min. The pyrolysis of SCG with the fats was seen to produce a liquid product with higher energy density and aliphatic content compared with defatted SCG pyrolysis.[11] The liquid products were described as straight and branched hydrocarbons, oxygenates, and nitrogenates. Vardon et al. concluded that the quality of liquid products from SCG pyrolysis was superior to that of the defatted SCG. Another investigation of the pyrolysis of SCG was performed by Kan et al.,[13] who studied *in situ* upgrading with a NiCu/γ-Al_2O_3 catalyst. It was concluded that the catalytic activity enhanced the production of CO, CO_2, and C_xH_y and altered the pyrolysis liquid product distribution.[13] Long carboxylic acids including palmitic acid, linoleic acid, and stearic acid, were found in the liquid product.[13]

Table 1: Characterization of the supported ZSM-5 catalyst (ρ_{bulk}: bulk density; d_p: particle diameter; S_{total}: total surface area; S_{micro}: micropore surface area; V_{micro}: pore volume; B.s.: Brønsted acidity; L.s.: Lewis acidity).

Physical Property	ρ_{bulk} (kg/m^3)	d_p (μm)	
	800	75~175	
Porosity Analysis	S_{total} (m^2/gr)	S_{micro} (m^2/gr)	V_{micro} (cm^3/gr)
	124.3	98.98	0.0461
Acidity Analysis	B.s. (μmol/gr)	L.s. (μmol/gr)	B.s./L.s.
	214.3	25.2	8.5

In summary, pyrolysis of SCG was shown to be effective in generating straight hydrocarbons, phenols, furans, carboxylic acids, and ketones,[11–13] but the resulting bio-oil required further upgrading and processing. In this study, a commercial ZSM-5 catalyst is used to facilitate the pyrolysis process conversion of oxygenates to olefins and aromatic hydrocarbons via dehydration and decarbonylation reactions. ZSM-5 has been shown most effective in upgrading liquid pyrolysis products of woody biomass to aromatic hydrocarbons through deoxygenation reactions.[1,14] The aforementioned studies indicate that the bio-oil product from SCG pyrolysis consists of heteroatomic oxygenated structures that can be upgraded to aromatic hydrocarbons with the use of a ZSM-5 catalyst, deeming it a promising candidate for chemicals production through catalytic pyrolysis. In this study, SCG valorization was achieved through pyrolysis at two heating rates: a moderate and a fast heating rate, both at short gas residence times. The focus of this work is to shed light to the reaction pathways that produce straight and aromatic hydrocarbons in the thermal and catalytic pyrolysis of SCG, and explore the potential benefits of catalytic upgrading and the temperature and heating rate effects on product selectivity to linear and aromatic hydrocarbons.

Materials and Methods

Materials

Wet spent coffee grounds (SCG) of mixed roasts were collected from a Starbucks coffee house in Mansfield, Connecticut. The wet SCG contained 60 wt% moisture content, and were dried for 24 hours at 378 K in a dry oven to remove the excess moisture. The particle size of the SCG was 180-355 μm. A commercial ZSM-5 catalyst from W. R. Grace & Co. was used in the catalytic experiments with properties as shown in Table 1. The acidity of the ZSM-5 catalyst was determined using Diffuse Reflectance Infrared Fourier Transform Spectroscopy (DRIFTS) and the surface area and pore size distribution were determined using N_2 physisorption.

Table 2: Elemental analysis by wt% of SCG compared with Miscanthus Giganteus from Du et al.[15] The fatty acids profile is shown as the relative composition by wt% of the total fat content in SCG. The total fat content was 10.89 wt% of the dry SCG feed. The C ##:# notation specifies the number of carbon atoms and the number of vinyl groups.

Elemental Analysis	SCG	Miscanthus Giganteus
Carbon	55.6	45.3
Hydrogen	7	5.8
Nitrogen	1.8	0.2
Oxygen (balance)	35.5	48.7
H/C_{eff} (mol% basis)	0.6	0
Fatty Acid Profile	Relative composition (wt%)	
Arachidic Acid (C 20:0)	2.74	
Linolenic Acid (C 18:3)	1.21	
Linoleic Acid (C 18:2)	42.05	
Oleic Acid (C 18:1)	9.32	
Stearic Acid (C 18:0)	7.59	
Palmitic Acid (C 16:0)	34.79	

Elemental analysis of the SCG was conducted in a Perkin-Elmer CHN2400 elemental analyzer. To provide some context, the elemental analysis of miscanthus giganteus from Du et al.[15] is compared with that of SCG in Table 2. Analysis of the total fat content and the fatty acid profile are also provided in Table 2. The dried SCG has greater carbon and hydrogen content and

lower oxygen content compared to miscanthus. The SCG contains 1.8 wt% nitrogen compared with 0.2 wt% nitrogen in miscanthus. One indicator of higher aromatic and olefin carbon selectivity from pyrolysis is the effective hydrogen to carbon ratio, H/C_{eff}, which was explored by Zhang et al.[16] and Noshadi et al.[17] Zhang et al. showed that the selectivity to aromatic hydrocarbons and olefins from ZSM-5-enhanced catalytic pyrolysis increased steeply as the H/C_{eff} increases from 0 to 1.2. In addition, the deactivation of the catalyst was seen to decrease with an increasing H/C_{eff} ratio. The H/C_{eff} of SCG is 0.6, which is greater than that of miscanthus, suggesting that the pyrolysis of SCG should be more selective to deoxygenated liquid products.

Fixed bed apparatus

SCG pyrolysis at a moderate heating rate was conducted in a fixed bed quartz reactor chamber (Figure 1). The bed volume for thermal experiments (including the biomass and downstream quartz wool) was 8 cm^3 and the bed volume for catalytic experiments (including biomass, catalyst, and quartz wool) was 11 cm^3. The residence time in the thermal bed was approximately 1.5 sec and residence time in the catalytic bed was approximately 2.5 sec. The process temperature was measured with a thermocouple placed inside the reaction bed. The average heating rate was measured to be 120 ± 20 K/min and was consistent across all pyrolysis temperatures. 1.0 gr of SCG and 1.0 gr of ZSM-5 (in catalytic experiments) were loaded into the reactor between the quartz wool layers. Prior to pyrolysis, the reactor was maintained in an inert Ar environment with a 100 mL/min purge. An impinger was filled with acetone and submerged in a dry ice bath, then placed at the reactor outlet to cool and condense the liquid products. The impinger outlet was connected to a 1 L gas bag for gas collection. The pyrolysis gas was analyzed off-line with a thermal conductivity detector gas chromatograph (GC-TCD), discussed in detail in the Analytical methods Section. During the heating stage, the reactor was elevated above the furnace which preheated the bed to 433 ± 20 K. To initiate pyrolysis, the bed was rapidly shifted into the center of the hot furnace. All of the visible vapors were observed to condense within 90 sec. The total time for the pyrolysis experiments was set to 5 min to ensure complete pyrolysis and stripping of the SCG. The reactor, impinger, and outlet nozzle were then weighed to determine the liquid yield. The reaction bed was also weighed to determine the char yield. The change in mass due to the evaporation of acetone was negligible. The liquid product was analyzed via gas chromatography mass spectrometry (GC-MS). The liquid product was collected by washing the reactor, impinger, and outlet nozzle with acetone. Therefore, only acetone soluble chemicals were measured in the liquid analysis. The gas yield was estimated by the difference between the mass of feed and the measured solid and liquid products. The accuracy of the product distribution was determined in repeatability tests in the fixed bed reactor, on the basis of which the experimental standard deviation was determined. The fixed bed experiments were repeated up to 3 times and the average standard deviation was 2.5 wt% for the liquid products, 1.4 wt% for the gas products, and 2.0 wt% for the solid yield.

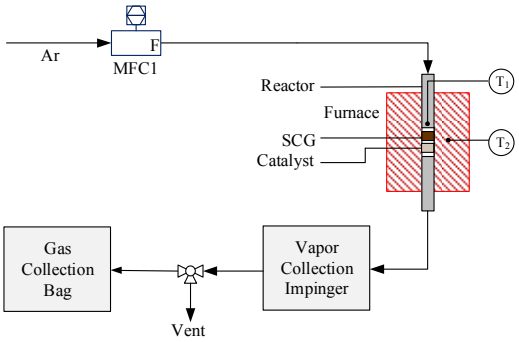

Figure 1: Schematic of the fixed bed reactor used for thermal and catalytic pyrolysis.

Pyroprobe apparatus

Fast pyrolysis was carried out in a CDS 5000 series Pyroprobe with a 0.013 cm^3 reactor volume and 0.07 sec of residence time. 10 mgr of SCG was packed into a 2.5 cm long quartz reactor vessel fixed between two quartz wool layers. In the catalytic experiments, ZSM-5 and SCG were mixed at a 1 to 1 mass ratio and 20 mg of mixture was loaded into the quartz reactor vessel. Pyrolysis was performed at 763 K, 813 K, and 863 K with a heating rate of 2000 K/sec, Ar flow rate of 10.5 mL/min, and 10 second dwell time. The condensable vapors were separated and analyzed online via GC-MS and the noncondensing gasses were analyzed online via mass spectrometry (MS). Post-pyrolysis, the reaction vessel was weighed to determine char yield. The SCG pyrolysis total liquid yield (including water) was estimated by taking the difference between the amount of SCG loaded and the gas and char yields. The pyroprobe experiments were repeated 3 times and the average standard deviation was 4.1 wt% for the liquid products, 1.6 wt% for the gas products, and 2.5 wt% for the solid yield.

Analytical methods

The SCG liquid pyrolysis products were analyzed in an Agilent 6890N Gas Chromatograph (GC) equipped with a 5973N mass selective detector (MS) and an Agilent DB-5 column. The GC oven started at 313 K, was held for 2 minutes, and then ramped to 543 K at 5 K/min. A 5 K/min heating rate was used for better compound separation in the chromatograph. Chemical species were identified by spectral comparison with the NIST mass spectral library. For the fixed bed experiments, mass quantification was achieved for palmitic acid, linoleic acid, and stearic acid. For the pyroprobe experiments, mass quantification was achieved for benzene, toluene, xylene, phenol, benzofuran, naphthalene, palmitic acid, linoleic acid, and stearic acid. Semi-quantification was implemented for the remaining aromatic species. All other species are reported by the percentages of the total peak area, and only their trends with respect to temperature and catalytic activity are of significance.

The fixed bed gas products were analyzed in an Agilent 6890N Gas Chromatograph (GC) equipped with a thermal conductivity detector (TCD) and a Restek ShinCarbon 19091J-413 column. 1 mL of gas was injected over 0.5 min with 373 K initial temperature and 1.9 mL/min flow. The temperature was held at 313 K for 2 min, increased to 393 K with a 2 K/min ramp, increased to 433 K with a 5 K/min ramp, and held at 433 K for 6 min. The CO, CO_2, H_2, and CH_4 outlet gas products from the pyroprobe experiments were quantified with a Mass Spectrometer calibrated with a synthesis gas standard.

Acid site densities of the original and used ZSM-5 catalysts were measured using DRIFTS. Used ZSM-5 catalyst was collected after the pyrolysis of SCG in the fixed bed reactor and was regenerated by burning off the coke at 1073 K. DRIFTS was performed at 393 K with KBr as background. Fresh and used ZSM-5 were calcined in N_2 at 823 K for 1 hr in the DRIFTS cell. The cell was then cooled down to 393 K. Pyridine was introduced into the sample cell under the N_2 flow. The FTIR spectrum was monitored until full saturation of pyridine on the sample occurred. Physisorbed pyridine was removed by heating the samples to 503 K for 1 hour. After that, the cell was cooled down again to 393 K. The FTIR spectrum was collected and used for the measurement of Brønsted (1550 cm^{-1}) and Lewis (1450 cm^{-1}) acid sites. Extinction coefficients of 1.67 cm/μmol and 2.22 cm/μmol were used for concentration calculation of Brønsted and Lewis acid sites, respectively.[14]

The pore size distribution and surface area of the original and regenerated catalyst samples were measured using the Barrett-Joyner-Halenda (BJH) method in a Micrometitics ASAP 2020 Accelerated Surface Area and Porosimetry System. Prior to analysis, the catalyst was degassed at 523 K for 12 hr under vacuum. N_2 physisorption isotherms were then measured at 77K to determine the physical properties of the catalyst.

Reaction Pathways

This section draws parallels between the pyrolysis of spent coffee grounds (SCG) and the pyrolysis of other biomass in order to illustrate the anticipated reaction pathways and justify the use of a ZSM-5 catalyst for *in situ* catalytic upgrading. These reaction pathways, mostly derived from the literature, will be used later to explain the product distribution of pyrolysis liquid products. The chemical composition of SCG can be categorized as protein, lignin, hemicellulose, cellulose, and lipids.[10,18] In contrast, lignocellulosic biomass (woody or agricultural[15,19]) is composed of hemicellulose, cellulose, and lignin. Pyrolysis depolymerizes and fragments these lignocellulosic structures into water, phenols, furans, cyclic ketones, and other heteroatomic structures.[19–21]

Many products similar to those of lignocellulosic biomass pyrolysis were generated in the pyrolysis of SCG studied by Vardon et al.,[11] Bok et al.,[12] and Kan et al.[13] A ZSM-5 catalyst is often included in the biomass pyrolysis process to enhance dehydration, decarboxylation, isomerization, and decarbonylation, thus increasing the selectivity to aromatic hydrocarbons and olefins.[22] This same approach is followed here in the pyrolysis of SCG to explore their selectivity to deoxygenated products and high-value chemicals. This section focuses only on the pyrolysis of lipids and proteins since the reaction pathways for the catalytic pyrolysis of lignocellulosic biomass is relatively well understood in the literature.[1,23,24]

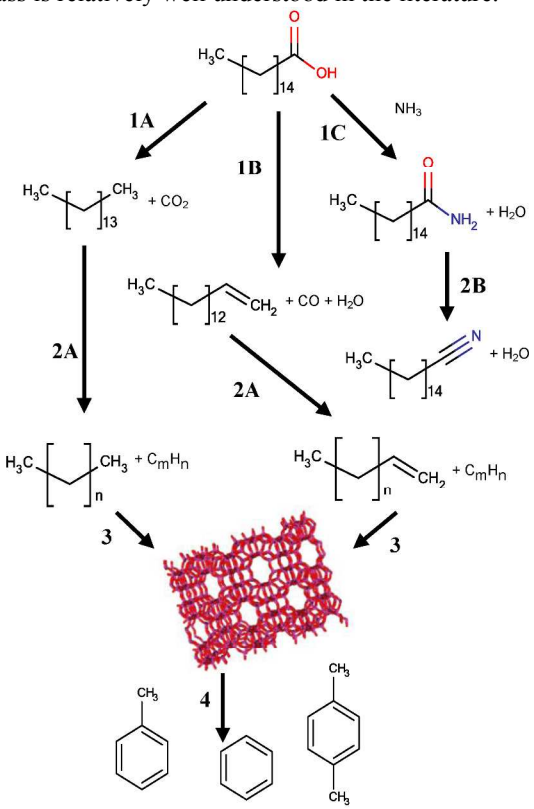

Scheme 1: Reaction pathway for triglycerides thermal and catalytic pyrolysis. The following reactions are illustrated: (1A) decarboxylation, (1B) decarbonylation, (1C) ammonia substitution, (2A) thermal cracking, (2B) amine pyrolysis, (3) catalytic cracking, (4) oligomerization, cyclization, and aromatization.

Lipid pyrolysis of SCG

The fat content in the SCG feedstock was measured to be 10.89 wt% of dry SCG feed (Table 2). The fatty acid groups in the SCG were linoleic acid (42.05 wt%), oleic acid (9.32 wt%), stearic acid (7.59 wt%), and palmitic acid (34.79 wt%). The main source of fatty acids in SCG are triglycerides[25] which pyrolyze to free fatty acids. These fatty acids are liberated from triglycerides through hydrolysis[26,27] or β-elimination.[27–29] The two primary pathways for fatty acid pyrolysis include decarboxylation and decarbonylation, as shown in the saturated fatty acid and vegetable oil pyrolysis studies of Gosselink et al.,[27] Maher et al.,[29,30] and Kubátová et al.[31] For the purpose of illustration, the palmitic acid pathway is presented in Scheme 1, since it is among the dominant primary products from SCG pyrolysis. The decarboxylation of palmitic acid produces pentadecane (Scheme 1, reaction 1A). Alternatively, the decarbonylation of palmitic acid produces 1-pentadecene (Scheme 1, reaction 1B). These reactions can also occur with stearic acid to produce heptadecane and 1-heptadecene. These

hydrocarbons thermally crack to shorter alkanes and alkenes (Scheme 1, reaction 2A). With the inclusion of a ZSM-5 catalyst, alkenes and alkanes can be branched to produce short olefins, and thereafter xylene and toluene via oligomerization, cyclization, and aromatization (Scheme 1, reaction 4). This mechanism has been proposed in the literature for the pyrolysis of fatty acids as well as alkanes.[32–34] In summary, the lipids found in SCG should pyrolyze to form long 1-alkenes and alkanes, and ZSM-5 catalytic pyrolysis will facilitate aromatization of straight hydrocarbons into cyclic structures.

Protein Pyrolysis of SCG

Catalytic pyrolysis of proteinaceous biomass has been explored in the literature. Mullen et al.[34] studied the pyrolysis of microalgae and egg whites with ZSM-5 and produced phenols, benzene, toluene, xylene, and other aromatics. Ammonia and other amines have been reported as products from the pyrolysis of proteinaceous biomass.[35–37] These nitrogen containing compounds can react with carboxylic acids to form amines,[38] (Scheme 1, reaction 1C) which can pyrolyze further to form nitriles.[39] (Scheme 1, reaction 2B)

Results and Discussion

Total liquid yield and product identification

The pyrolysis of SCG in the fixed bed reactor produced a liquid product consisting of furans, phenols, aromatic hydrocarbons, linear hydrocarbons, caffeine, fatty acids, nitriles, amides, among other compounds, with a total liquid yield of 51-58 wt% (Figure 2a). For illustration purposes, the liquid products were categorized in functional groups as ketones, oxygenated and nitrogenated aromatics, aromatic hydrocarbons, alkenes and alkanes, and fatty acids (Figure 3a). A detailed liquid product distribution can be found in the Supporting Information (Tables S1 and S2). The relative abundance of aromatic hydrocarbons, alkenes, and alkanes increased with temperature in both thermal and catalytic experiments (Figure 3a), while the selectivity to fatty acids (Figure 3b) was found to decrease with increasing temperature.

The pyroprobe liquid product was comparable in composition to that of the fixed bed containing furans, phenols, aromatic hydrocarbons, linear hydrocarbons, caffeine, fatty acids, nitriles, and amides with a total liquid yield of 35-42 wt% (Figure 2b). Moreover, the faster heating rate of the pyroprobe and its better separation of liquid products during GC-MS analysis showed other products such as pyridines, benzylnitrile, butynylbenzene, cyclododecane, cyclododecyne, hexadecanoic methyl ester, and 10,12-hexadecadienal (Table S2). These products were also categorized in their functional groups (Figure 4a).

Liquid selectivity

Fate of fatty acids: Palmitic acid, stearic acid, and linoleic acid were measured in the liquid product from the pyrolysis of spent coffee grounds at both heating rates. From the fixed bed, the selectivity to these fatty acids was seen to decrease with an increase in pyrolysis temperature (Figures 3b). Conversely, the selectivity to alkenes and alkanes increased with temperature (Figures 3a). Presumably, alkanes and 1-alkenes were formed via decarboxylation and decarbonylation of the saturated fatty acids, palmitic and stearic acid (Scheme 1, reactions 1A and 1B). The decarboxylation of linoleic acid and oleic acid can produce n-alkenes, yet these were mostly absent in the SCG pyrolysis experiments. Alkanes and 1-alkenes were the predominant linear hydrocarbons found in the liquid product at both heating rates. In addition, the selectivity to stearic acid from the fixed bed pyrolysis was particularly high (Figure 3b), which indicates that the saturation of linoleic acid and oleic acid to stearic acid via hydrogenation occurred as the first step in pyrolysis and that the chemistry of saturated fatty acids was dominant in SCG pyrolysis. The same saturation behavior was observed in the pyrolysis of linoleic acid conducted by Asomaning et al.,[40] who reported that there was a greater selectivity to 1-heptadecene and heptadecane than 8-heptadecene and other n-heptadecenes with double bonds corresponding to the position of the double bonds in the reactant fatty acid. This saturation behavior appeared to be dominant in the pyrolysis of SCG in the fixed bed, yet 8-heptadecene was identified in the liquid product from the pyroprobe pyrolysis experiments, likely as a result of decarboxylation of linoleic acid without complete saturation.

The decarboxylation of fatty acids to form alkanes (Scheme 1, reaction 1A) and the decarbonylation of fatty acids to form 1-alkenes (Scheme 1, reaction 1B) competed during the pyrolysis of SCG. The selectivity to 1-heptadecene and 1-pentadecene was lower than the selectivity to heptadecane and pentadecane at both heating rates, which suggests that decarboxylation was the primary pathway for fatty acid decomposition. From Figure 3a it can be seen that in the fixed bed the selectivities to alkanes and alkenes increased with increasing temperature in both thermal and catalytic experiments. No clear trend with temperature was observed in the pyroprobe. The effect of the ZSM-5 catalyst was seen to decrease the selectivity to alkenes and alkanes at both heating rates (Figure 3a and 4a). These products were oligomerized to aromatic hydrocarbons (Figure 4b) due to the positive effect of ZSM-5 on aromatic hydrocarbons selectivity. The selectivity to fatty acids in the pyroprobe liquid products was at highest at 17.2 wt%, comparable to the selectivity to fatty acids in the fixed bed.

Formation of aromatics: The ZSM-5 catalyst had a clear effect on the selectivity to O,N aromatics (furans, pyridines, phenols, indoles, etc.) and aromatic hydrocarbons (benzene, toluene, xylene, etc.). The selectivity to O,N aromatics was substantially higher in thermal experiments when compared with the catalytic experiments at both heating rates. In contrast, the selectivity to aromatic hydrocarbons is substantially greater in catalytic experiments when compared with thermal experiments at both heating rates. This trend is clearly illustrated in Figures 3a and 4a when comparing thermal and catalytic experiments at each temperature. Figure 4b shows the

liquid selectivity to aromatic hydrocarbons, furans, and phenols from the pyroprobe pyrolysis experiments. Aromatic hydrocarbon production increased tenfold with the inclusion of the ZSM-5 catalyst from 0.1-0.2 wt% in thermal pyrolysis to 2.3-2.9 wt% in catalytic pyrolysis. On the other hand, the selectivity to furans was seen to decrease from 0.3-0.4 wt% in thermal pyrolysis to ~0.1 wt% in catalytic experiments. Thus, the ZSM-5 catalyst was seen to significantly enhance selectivity to aromatic hydrocarbons and decrease selectivity to furans. This finding is consistent with the work by Cheng et al.,[22] who observed that catalytic pyrolysis with a ZSM-5 catalyst can convert furans to aromatic hydrocarbons.

Increasing the pyrolysis temperature was seen to have a positive effect on the selectivity to aromatic hydrocarbons in the fixed bed. The selectivity to aromatic hydrocarbons from catalytic pyrolysis in the fixed bed was seen to increase threefold, when the temperature was increased from 763-863 K (Figure 3a). The selectivity to aromatic hydrocarbons was seen to decrease with increasing temperature in the pyroprobe. This is attributed to the lipids present in SCG. For instance, in the pyrolysis of canola oil, which contains similar fatty acids to SCG, performed by Du et al.[34] and Katikaneni et al.,[41] a decreasing selectivity to aromatic hydrocarbons was observed with increasing temperature, in favor of coke formation. Overall, the selectivity to aromatic hydrocarbons was seen to increase with increasing temperature (in the fixed bed) and with the ZSM-5 catalyst.

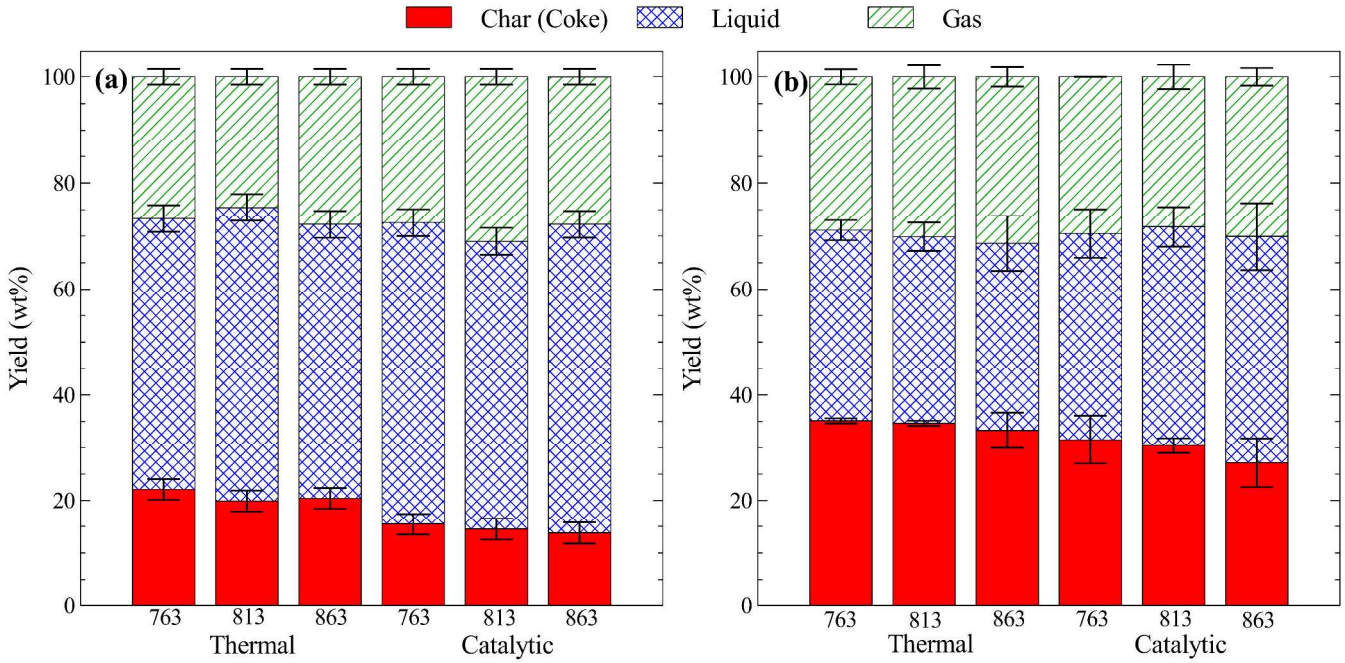

Figure 2: Total product yields by wt% for the fixed bed (a) and pyroprobe (b). The gas yield from fixed bed and liquid yield from pyroprobe pyrolysis experiments were calculated by difference.

Alkene and alkane intermediates: C_{13} to C_{17} linear hydrocarbons were produced by fatty acid pyrolysis. The selectivity to linear hydrocarbons in the fixed bed increased with temperature by twofold in thermal experiments and by threefold in catalytic experiments (Figure 3a). The experiments with ZSM-5 were less selective to straight hydrocarbons due to catalytic cracking and branching. The pyroprobe results verified the cracking behavior, as shown in Figure 4a. The ZSM-5 catalyst was seen to increase selectivity to xylene, toluene, naphthalene, benzene, and styrene at the expense of linear hydrocarbons. The ZSM-5 catalyst promoted oligomerization, cyclization, and aromatization reactions of straight paraffins and olefins (Scheme 1, reaction 4).

Nitrogen containing liquid products: Nitrogen was found in SCG pyrolysis liquid products in the form of caffeine, hexadecanitrile, hexadecaneamide, benzylnitrile, pyridine, and indole derivatives. SCG has a sizable protein content[18] which is a source of nitrogen in addition to caffeine. Hexadecanamide was observed in the pyrolysis of SCG in the fixed bed, which suggests that palmitic acid underwent an amidization reaction with ammonia (Scheme 1, reaction 1C). In addition, the existence of hexadecanitrile is evidence of the amide pyrolysis reaction (Scheme 1, reaction 2B). Previous studies involving proteinaceous biomass performed by Mullen et al.[37] reported ammonia and amide products. The co-existence of amides, nitriles, alkanes, and 1-alkenes indicates that ammonia substitution, decarbonylation, and decarboxylation are all possible pathways for fatty acid pyrolysis. In addition, hexadecanamide was measured in the liquid products from fixed bed experiments but not from the pyroprobe experiments. This suggests that due to the faster heating rate, the pyrolysis of hexadecanamide went to completion in the pyroprobe to produce hexadecanenitrile.

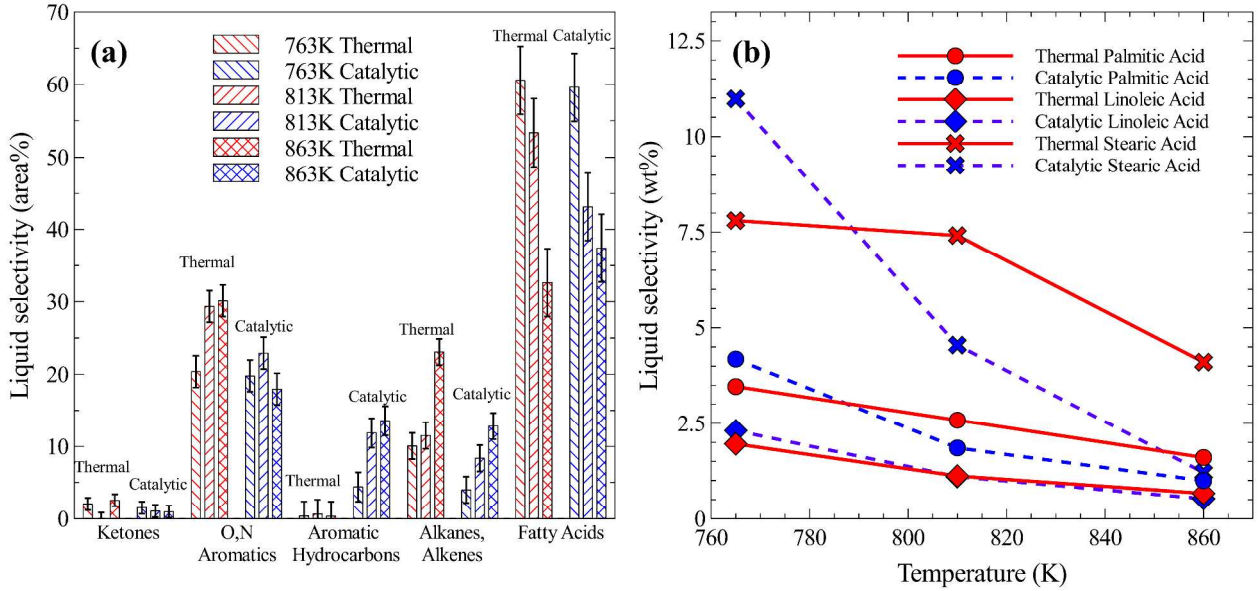

Figure 3: Fixed bed liquid selectivity by GC-MS area% (a); and selectivity to fatty acids by wt% (b) for thermal experiments (red) and catalytic experiments (blue). In Figures 3 and 4 the selectivity by area% is defined by the quotient of the area of the peak in the GC-MS chromatograph divided by the total area of identified species. The selectivity by wt% is defined by the quotient of the mass of the measured species divided by the total mass of the liquid product.

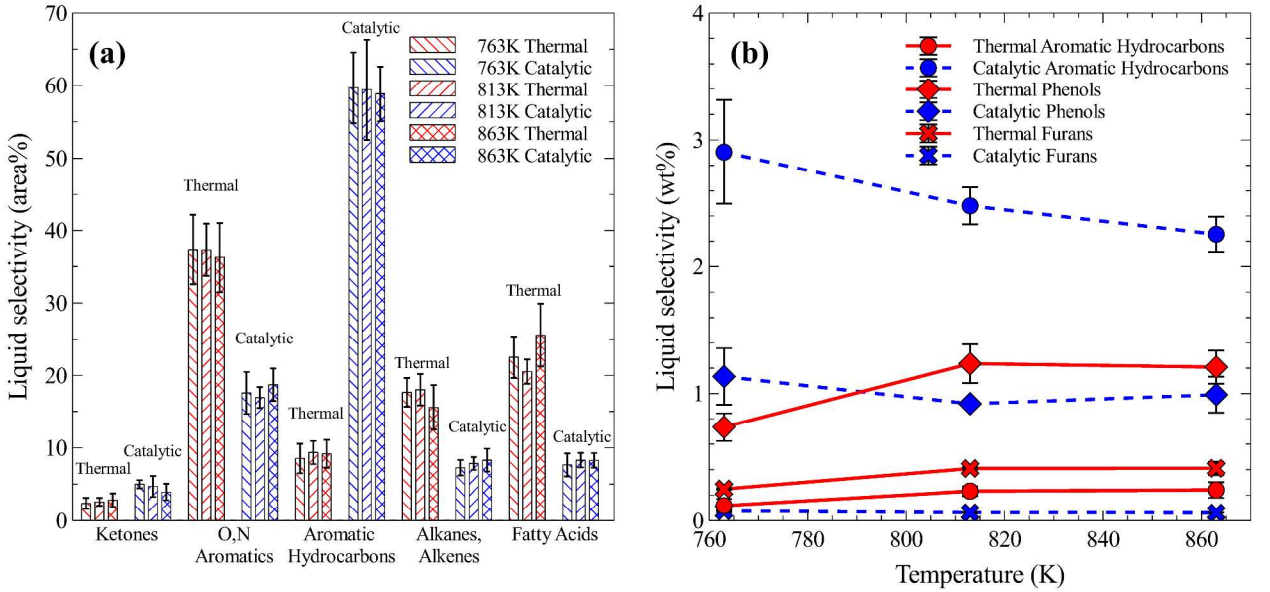

Figure 4: Pyroprobe liquid selectivity by GC-MS peak area% (a) and selectivity to aromatic hydrocarbons, phenols, and furans by wt% (b) for thermal experiments (red) and catalytic experiments (blue). The selectivity by wt% to fatty acids (not shown here) was found in the range 9.7-17.2 wt% for the thermal experiments and 7.9-8.2 wt% for the catalytic experiments.

Gas Product Distribution

The gas yields from the pyrolysis of SCG in the fixed bed and pyroprobe are shown in Figure 5. The yield to CO from the thermal pyrolysis of SCG in the fixed bed was 10.5-12 wt%. The yield to CO from the catalytic pyrolysis of SCG in the fixed bed was 11.5-13 wt%, increased by 1 wt% from thermal pyrolysis. The gas product from the pyroprobe showed a similar increase in CO production. The CO yield from thermal pyrolysis experiments was 6.1-6.5 wt%, while the yield from catalytic pyrolysis experiments was 7.8-8 wt%. The increase in CO yield between thermal and catalytic experiments can be explained with the ZSM-5 promoted decarbonylation reactions. The yield to CO_2 from thermal pyrolysis in the fixed bed was 12.0-14.0 wt% while the CO_2 yield from catalytic pyrolysis in the fixed bed was 12.5-14.5 wt%. The CO_2 yield from thermal pyrolysis in the pyroprobe was 20.9-23.7 wt% and the CO_2 yield from the catalytic pyrolysis was 19.3-21.1 wt%. There is no clear effect of the ZSM-5 catalyst on the CO_2 yield. At both heating rates, the high CO_2 yield is partially due to thermal decarboxylation reactions of palmitic, linoleic, and stearic

acids. The yield to CH_4 from thermal fixed bed pyrolysis was 2.5-4 wt% and the yield of CH_4 from catalytic pyrolysis was 1.5-2.5 wt%. The CH_4 yield was 1.1-1.4 wt% in the pyroprobe for both thermal and catalytic pyrolysis. The substantial CH_4 yield is evidence of thermal cracking mechanisms that produce small fragmented alkanes during pyrolysis. ZSM-5 was seen to lower the CH_4 yield, which suggests that ZSM-5 catalyzed oligomerization reactions of the CH_4 precursors to form aromatic hydrocarbons. The hydrogen yield from thermal pyrolysis in the fixed bed was 0.5-1 wt% and the hydrogen yield from catalytic pyrolysis in the fixed bed was 0.2-0.5 wt%, yet was negligible in the pyroprobe experiments. The lack of hydrogen from the pyroprobe experiments helps to explain the 8-heptadecane found in the liquid product as a result of incomplete saturation of the linoleic acid. The CO to CO_2 ratio is much higher in the fixed bed than the pyroprobe. This is a result of the decarbonylation of fatty acids being favored in the fixed bed as indicated by a greater selectivity to 1-alkenes in the fixed bed than in the pyroprobe (Table S1 and S2). In addition, the pyrolysis of SCG in the pyroprobe had a greater selectivity to phenols than in the fixed bed (Table S1 and S2), which indicates that phenols were more reactive in the fixed bed to produce CO via decarbonylation reactions. Responses for NH_3, NO, and HCN were also detected, but not quantified. The overall effects of using a ZSM-5 catalyst on the gas yields in SCG pyrolysis can be seen by an increase in CO yield under catalytic conditions due to decarbonylation reactions at both heating rates and a decrease in CH_4 yield in the fixed bed due to enhancement of catalytic oligomerization reactions.

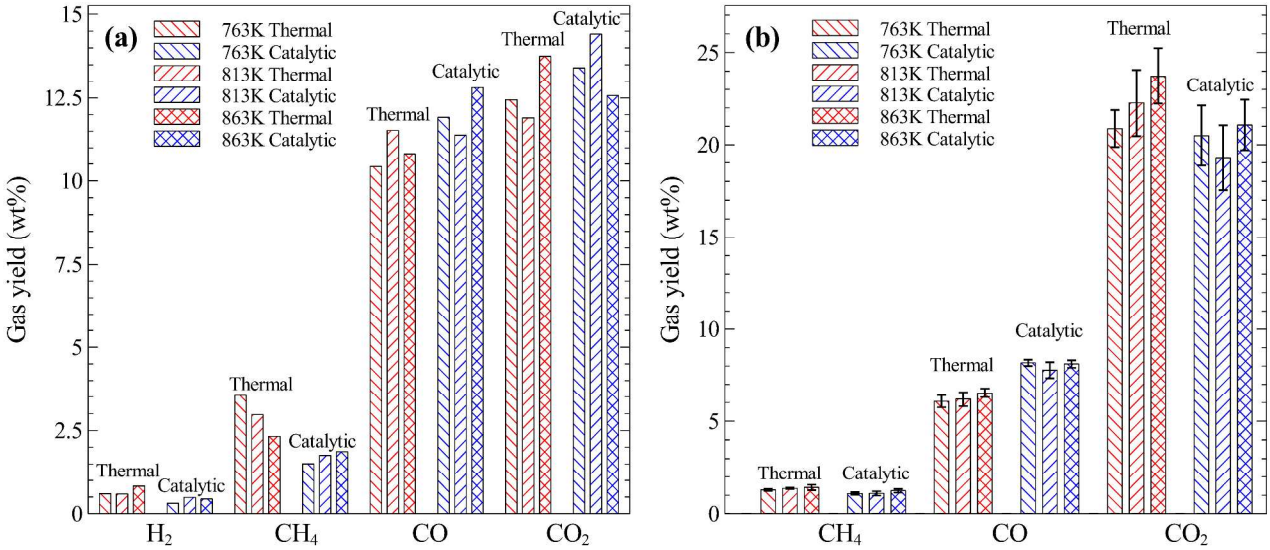

Figure 5: H_2, CH_4, CO, and CO_2 gas yield (wt%) from fixed bed thermal and catalytic experiments (a) and pyroprobe thermal and catalytic experiments (b).

Char analysis and catalyst activity

Solid yields from the pyrolysis of SCG in the fixed bed were measured at 15-20 wt%. The elemental analysis of the SCG feedstock and thermal biochars of the fixed bed pyrolysis experiments is reported in Table 3. Nitrogen, carbon, and sulfur content were significantly greater in the char samples than in SCG. In contrast, hydrogen and oxygen were dramatically decreased, showing that hydrogen and oxygen sources are more readily pyrolyzed than carbon, nitrogen, and sulfur. Increasing the pyrolysis temperature was seen to increase the char carbon content, while the hydrogen and oxygen content was seen to decrease. The effect of temperature on the overall coke and char yields was not clear. On the other hand, the solid yield was seen to be lower in catalytic experiments (coke) than in thermal experiments (char) at both heating rates (Figure 2). The pyrolysis of SCG in the pyroprobe was seen to generate twice the solid product by wt% than the fixed bed. This is a result of the difference between the *in situ* catalyst loading in the pyroprobe and *ex situ* catalyst loading in the fixed bed. The *in situ* method results in lower rates of mass transfer, direct mixing of coke precursors with the catalyst, and enhanced coke formation.[9] Wang et al.[9] reports a similar discrepancy in total solids yield when comparing *in situ* and *ex situ* pyrolysis. In addition, one third of the nitrogen found in the SCG was retained in the biochar. The increased nitrogen content suggests that the char product from an industrial scale process with an *ex situ* catalytic upgrading step downstream the SCG pyrolysis process, may be used as a low quality fertilizer. From an environmental point of view, the retention of nitrogen and sulfur in the solid residue is a clear advantage of SCG pyrolysis as compared to the combustion and gasification of these elements.

The acidity of the ZSM-5 catalyst before and after one catalytic experiment was explored in order to provide an indication of the catalyst stability in SCG pyrolysis. The acidity of the Brønsted acid sites was seen to decrease from 214.3 μmol/gr in the original catalyst to 191.8 μmol/gr in the recovered catalyst. Water is produced in many pyrolysis

reactions and contributes to the loss of Brønsted acid sites as a result of dealumination of the zeolite framework.[5] The loss of Brønsted sites is also likely attributed to potassium generally found in SCG.[6] The acidity of the Lewis sites was seen to decrease from 25.2 μmol/gr in the original catalyst to 19.0 μmol/gr in the recovered catalyst. The ratio of Brønsted acid to Lewis acid sites increased from 8.5 μmol/gr in the original catalyst to 10.1 μmol/gr in the recovered catalyst. Overall, a decrease in the acidity of the ZSM-5 catalyst was observed after use in the pyrolysis of SCG.

Table 3: Elemental analysis of fixed bed thermal chars and SCG feedstock (wt%).

	SCG	Thermal char		
		763K	813K	863K
Carbon	55.6	72.0	74.8	76.2
Hydrogen	7.0	3.7	3.0	2.5
Nitrogen	1.8	2.9	3.0	2.9
Oxygen	35.5	21.1	18.9	18.8
Sulfur	0.2	0.4	0.4	0.3

Conclusions

The pyrolysis of spent coffee grounds in fixed bed and pyroprobe thermal and catalytic experiments produced a liquid product containing phenols, pyridines, furans, fatty acids, linear hydrocarbons, and aromatic hydrocarbons. The fatty acids pyrolyzed mainly through decarboxylation and decarbonylation reactions. Pyrolysis with a commercial ZSM-5 catalyst was seen to enhance the selectivity of the liquid product to aromatic hydrocarbons, including benzene, xylene, and toluene, despite the low biomass to catalyst ratio. ZSM-5 catalyzed oligomerization, cyclization, and aromatization reactions of straight paraffins and olefins to benzene and xylene. The ZSM-5 catalyst increased the CO yield, formed via decarbonylation reactions. In addition, higher temperatures promoted the conversion of SCG to hydrocarbon products. These temperature and catalytic trends were consistent across both heating rates. One third of the nitrogen in SCG feed was retained in the char, indicating its potential use as a fertilizer.

Acknowledgements

This work was supported by the IDEA Grant of the University of Connecticut Office of Undergraduate Research. Coffee waste was donated by the Starbucks Coffee Company branch located in Mansfield Connecticut. Catalyst was provided by W. R. Grace & Co. AF was partially sponsored by the Udall Foundation for environmental research. SD and JAV acknowledge the support by the National Science Foundation under Grant No. CBET 1236738.

Notes and references

Department of Chemical & Biomolecular Engineering, University of Connecticut, Storrs, 191 Auditorium Road, Unit 3222, Storrs, CT 06269-3222, USA.

* These authors contributed equally to the work.

† Corresponding Author: E-mail: george.bollas@uconn.edu; Tel: +1-860-486-4602

Electronic Supplementary Information (ESI) available: GC-MS chromatograph area percentage report for liquid analysis of the fixed bed and pyroprobe bio-oil. See DOI: 10.1039/b000000x/

1 T. R. Carlson, G. A. Tompsett, W. C. Conner and G. W. Huber, *Top. Catal.*, 2009, **52**, 241–252.
2 M. S. Mettler, D. G. Vlachos and P. J. Dauenhauer, *Energy Environ. Sci.*, 2012, **5**, 7797.
3 N. Kondamudi, S. K. Mohapatra and M. Misra, *J. Agric. Food Chem.*, 2008, **56**, 11757–11760.
4 *http://www.ico.org/.*
5 D. J. Wuebbles and K. Hayhoe, *Earth-Science Rev.*, 2002, **57**, 177–210.
6 M. R. Adams and J. Dougan, in *Coffee Technology*, eds. R. J. Clarke and R. Macrae, Elsevier Applied Science Publishers Ltd., New York, 1987, pp. 257–291.
7 A. Sampaio, G. Dragone, M. Vilanova, J. M. Oliveira, J. A. Teixeira and S. I. Mussatto, *LWT - Food Sci. Technol.*, 2013, **54**, 557–563.
8 M. A. Silva, S. A. Nebra, M. J. Silva, Machado and C. G. Sanchez, *Biomass and Bioenergy*, 1998, **14**, 457–467.
9 G. Xu, T. Murakami, T. Suda, Y. Matsuzawa and H. Tani, *Energy & Fuels*, 2006, **20**, 2695–2704.
10 S. A. Franca and L. S. Oliveira, in *Agricultural Wastes*, eds. G. S. Ashworth and P. Azevedo, Nova Science Publishers, Inc., Belo Horizonte Brazil, 2009, pp. 155–189.
11 D. R. Vardon, B. R. Moser, W. Zheng, K. Witkin, R. L. Evangelista, T. J. Strathmann, K. Rajagopalan and B. K. Sharma, *ACS Sustain. Chem. Eng.*, 2013, **1**, 1286–1294.
12 J. P. Bok, H. S. Choi, Y. S. Choi, H. C. Park and S. J. Kim, *Energy*, 2012, **47**, 17–24.
13 T. Kan, V. Strezov and T. Evans, *Energy & Fuels*, 2014, **28**, 228–235.
14 E. F. Iliopoulou, S. D. Stefanidis, K. G. Kalogiannis, A. Delimitis, A. A. Lappas and K. S. Triantafyllidis, *Appl. Catal. B Environ.*, 2012, **127**, 281–290.
15 S. Du, Y. Sun, D. P. Gamliel, J. A. Valla and G. M. Bollas, *Bioresour. Technol.*, 2014, **169**, 188–197.
16 H. Zhang, Y.-T. Cheng, T. P. Vispute, R. Xiao and G. W. Huber, *Energy Environ. Sci.*, 2011, **4**, 2297–2307.
17 I. Noshadi, B. Kanjilal, S. Du, G. M. Bollas, S. L. Suib, A. Provatas, F. Liu and R. S. Parnas, *Appl. Energy*, 2014, **129**, 112–122.
18 S. I. Mussatto, E. M. S. Machado, S. Martins and J. A. Teixeira, *Food Bioprocess Technol.*, 2011, **4**, 661–672.
19 D. Mohan, C. U. Pittman, and P. H. Steele, *Energy & Fuels*, 2006, **20**, 848–889.
20 P. R. Patwardhan, D. L. Dalluge, B. H. Shanks and R. C. Brown, *Bioresour. Technol.*, 2011, **102**, 5265–9.
21 P. R. Patwardhan, R. C. Brown and B. H. Shanks, *ChemSusChem*, 2011, **4**, 1629–1636.
22 Y.-T. Cheng and G. W. Huber, *Green Chem.*, 2012, **14**, 3114–3125.
23 A. Aho, N. Kumar, K. Eränen, T. Salmi, M. Hupa and D. Y. Murzin, *Fuel*, 2008, **87**, 2493–2501.
24 J. Jae, G. A. Tompsett, A. J. Foster, K. D. Hammond, S. M. Auerbach, R. F. Lobo and G. W. Huber, *J. Catal.*, 2011, **279**, 257–268.
25 K. Speer and I. Kölling-Speer, *Brazilian J. Plant Physiol.*, 2006, **18**, 201–216.
26 B. Donnis, R. G. Egeberg, P. Blom and K. G. Knudsen, *Top. Catal.*, 2009, **52**, 229–240.
27 R. W. Gosselink, S. A. W. Hollak, S.-W. Chang, J. van Haveren, K. P. de Jong, J. H. Bitter and D. S. van Es, *ChemSusChem*, 2013, **6**, 1576–1594.
28 C. D. Hurd and F. H. Blunck, *J. Am. Chem. Soc.*, 1938, **118**, 2419–2425.
29 K. D. Maher, K. M. Kirkwood, M. R. Gray and D. C. Bressler, *Ind. Eng. Chem. Res.*, 2008, **47**, 5328–5336.
30 K. D. Maher and D. C. Bressler, *Bioresour. Technol.*, 2007, **98**, 2351–2368.
31 A. Kubátová, Y. Luo, J. Šťávová, S. M. Sadrameli, T. Aulich, E. Kozliak and W. Seames, *Fuel*, 2011, **90**, 2598–2608.
32 N. Mo and P. E. Savage, *ACS Sustain. Chem. Eng.*, 2014, **2**, 88–94.

33 P. V. Lipin, V. P. Doronin and T. I. Gulyaeva, *Pet. Chem.*, 2010, **50**, 362–367.
34 Z. Du, B. Hu, X. Ma, Y. Cheng, Y. Liu, X. Lin, Y. Wan, H. Lei, P. Chen and R. Ruan, *Bioresour. Technol.*, 2013, **130**, 777–782.
35 K.-M. Hansson, J. Samuelsson, C. Tullin and L.-E. Åmand, *Combust. Flame*, 2004, **137**, 265–277.
36 S. Yuan, Z. Zhou, J. Li, X. Chen and F. Wang, *Energy & Fuels*, 2010, **24**, 6166–6171.
37 C. A. Mullen and A. A. Boateng, *BioEnergy Res.*, 2011, **4**, 303–311.
38 D. P. N. Satchell and R. S. Satchell, in *The Chemistry of Carboxylic Acids and Esters*, ed. S. Patai, John Wiley & Sons, Ltd., Chichester, UK, 2010, pp. 375–452.
39 J. F. Bieron, F. J. Dinan and J. Dinan, in *Amides (1970)*, ed. J. Zabicky, John Wiley & Sons, Ltd., Chichester, UK, 2010, pp. 245–288.
40 J. Asomaning, P. Mussone and D. C. Bressler, *Fuel Process. Technol.*, 2014, **120**, 89–95.
41 S. P. R. Katikaneni, J. D. Adjaye, R. O. Idem and N. N. Bakhshi, *J. Am. Oil Chem. Soc.*, 1998, **75**, 381–391.
42 K. Wang, P. A. Johnston and R. C. Brown, *Bioresour. Technol.*, 2014, **173**, 124–31.
43 J. L. Tallon and R. G. Buckley, *J. Phys. Chem.*, 1987, **91**, 1469–1475.
44 A. López, I. de Marco, B. M. Caballero, A. Adrados and M. F. Laresgoiti, *Waste Manag.*, 2011, **31**, 1852–8.
45 S. Du, J. A. Valla and G. M. Bollas, *Green Chem.*, 2013, **15**, 3214.
46 T. Blasco, a Corma and J. Martineztriguero, *J. Catal.*, 2006, **237**, 267–277.
47 P. Pohl, E. Stelmach, M. Welna and A. Szymczycha-Madeja, *Food Anal. Methods*, 2012, **6**, 598–613.

